

# Extended seasonal prediction of Antarctic sea ice concentration using ANTSIC-UNet

Ziying Yang<sup>1, 2, 5</sup>, Jiping Liu<sup>3</sup>, Mirong Song<sup>1</sup>, Yongyun Hu<sup>4</sup>, Qinghua Yang<sup>3</sup>, Ke Fan<sup>3</sup>, [Rune Grand Graversen<sup>5</sup>](#), [Lu Zhou<sup>6</sup>](#)

5 <sup>1</sup>Institute of Atmospheric Physics, Chinese Academy of Sciences, Beijing 100029, China

<sup>2</sup>University of Chinese Academy of Sciences, Beijing 101408, China

<sup>3</sup>School of Atmospheric Sciences, Sun Yat-sen University, and Southern Marine Science and Engineering Guangdong Laboratory (Zhuhai), Zhuhai 519082, China

10 <sup>4</sup>Department of Atmospheric and Oceanic Sciences, School of Physics, Peking University, Beijing 100087, China

<sup>5</sup>[Department of Physics and Technology, Arctic University of Norway, Tromsø 9019, Norway](#)

<sup>6</sup>[Institute for Marine and Atmospheric research Utrecht, Utrecht University, Utrecht 3584 CC, Netherlands](#)

Correspondence to: Jiping Liu (liupj63@mail.sysu.edu.cn)

**Abstract.** Antarctic sea ice has experienced rapid change in recent years, with the total sea ice extent abruptly decreasing after a period of gradual increase from the late 1970s until 2014. Accurate long-term predictions of Antarctic sea ice concentration are crucial for supporting expanding activities in the Southern Ocean, related to for instance scientific research, tourism and fisheries. However, dynamical models often face difficulties in accurately predicting Antarctic sea ice due to limited representations of air-ice-sea interactions, especially on seasonal timescales and during the summer months. In response to these challenges, we develop a deep learning model (named ANTSIC-UNet), trained by physically enriched climate variables, and evaluate its skill for extended up-to-six-months seasonal prediction of Antarctic sea ice concentration. We compare the predictive skill of ANTSIC-UNet in the Pan- and regional Antarctic with two benchmark models (a linear trend and an anomaly persistence model). In terms of root-mean-square error (RMSE) for sea ice concentration and integrated ice-edge error (IIIE), ANTSIC-UNet shows much better skills relative to the two benchmark models for the extended seasonal prediction, especially for the extreme events in recent years. Sea ice prediction errors increase with lead time, and are smaller during autumn and winter than in summer. The Pacific and Indian Oceans show accurate prediction performance at the sea ice edge during summer, and ANTSIC-UNet provides high predictive skill in capturing the interannual variability of Pan-Antarctic and regional sea ice extent anomalies. In addition, we quantify the importance of variables through a post-hoc interpretation method. This analysis suggests that the ANTSIC-UNet prediction at short lead times is sensitive to sea surface temperature, radiative flux, and atmospheric circulation in addition to sea ice conditions. At longer lead times, zonal wind in the stratosphere appears to be an important influencing factor for the prediction.

**Deleted:** which garners increasing attention for its prediction. In this study,

**Deleted:** (up to 6 months in advance).

**Deleted:** s

**Deleted:** , relative to the two benchmark models

**Deleted:** The predictive skill of ANTSIC-UNet is season and region dependent. Low values of RMSE are found from autumn to spring in the Pan-Antarctic and all sub-regions for all lead times, but large values of RMSE are found in summer for most sub-regions which increase as lead times increase. Small values of IIIE are found in summer at 1-3 month lead, large errors occur from November to January as the lead time exceeds 2-4 months.

**Deleted:** better predictive skills at the sea ice edge zone in summer compared to other regions. Moreover, ANTSIC-UNet shows good

**Deleted:** We also

**Deleted:** importance

**Deleted:** It

**Deleted:** in addition to sea ice conditions,

**Deleted:** shows

**Deleted:** sensitivity

50 1 Introduction

50 Sea ice affects the climate system through modulating the exchange of radiation, heat, momentum, moisture and gases between the atmosphere and ocean. Antarctic sea ice is an essential component of the climate system. It strongly affects the local atmosphere and ocean and the extrapolar Southern Hemisphere through dynamical and thermodynamic processes, particularly in a warming climate (Massom and Stammerjohn, 2010; Kidston et al., 2011; Abernathey et al., 2016; Zhu et al., 2023).

**Deleted:** , which

55 summer total Antarctic sea ice extent (SIE) has gradually increased until 2014 since the late 1970s and then abruptly decreased (Turner et al., 2013; Hobbs et al., 2016; Comiso et al., 2017; Fogt et al., 2022; Liu et al., 2023). Antarctic SIE shows large seasonal and interannual variability, with trends that are spatially heterogeneous (Liu et al., 2004; Raphael and Hobbs, 2014; Libera et al., 2022).

**Deleted:** sea ice

**Deleted:** and its trend is spatially

Compared to the Arctic, the prediction of Antarctic sea ice has received much less attention. Yet subseasonal to extended seasonal Antarctic sea ice predictions are increasingly demanded due to the expanding range of activities in the Southern Ocean (Zampieri et al., 2019; Bushuk et al., 2021; Libera et al., 2022). Accurate sea ice concentration predictions can provide early warnings about sea ice changes and related hazards. This is particularly important for managing the risks of shipping activities in the Southern Ocean. For example, two polar vessels, Akademik Shokalskiy and Xuelong became trapped in rapidly formed sea ice in the Antarctic coastal region (Wang et al., 2014). Commercial fishing and tourism operations mostly use ice-strengthened vessels rather than icebreakers, which are vulnerable to sea ice hazards. Improved predictions will support ecosystem management and inform policy decisions, since the seasonal variations in Antarctic sea ice have a profound influence on marine productivity and fisheries (Libera et al., 2022).

Statistical models, such as the Markov model (e.g., Chen and Yuan, 2004; Pei, 2021) and the Koopman mode decomposition model (Hogg et al., 2020), have been employed to forecast seasonal Antarctic sea ice concentration. However, these statistical

**Deleted:** , but it is also in demand associated with the increase in planning operational activities like scientific research, tourism, and fishing in the Southern Ocean (Bushuk et al., 2021; Libera et al., 2022)....

**Deleted:** In general

**Deleted:** There

70 models were inferior to the anomaly persistence model for some seasons and regions. Additionally, there have been limited efforts to forecast seasonal Antarctic sea ice using dynamical models due to the challenges associated with faithfully simulating complex air-ice-sea interaction processes in the Southern Ocean (Morioka et al., 2019; Bushuk et al., 2021). Dynamically, sea ice movement and deformation are driven by wind and ocean currents. Thermodynamically, sea ice melting and formation are influenced by convection associated with ocean vertical mixing, heat exchange driven by surface radiation budget and 75 turbulence, and heat advection through horizontal transport of air and water masses. However, most dynamical forecast systems overestimate the extent of the Antarctic sea ice edge at the sub-seasonal scale with their predictive skill falling below climatological benchmarks (Zampieri et al., 2019). Starting in 2017, the Sea Ice Prediction Network South (SIPN South) has coordinated the evaluation of forecasting methods and systems used to predict summer Antarctic sea ice (Massonnet et al., 2023). The evaluation reveals that both statistical and dynamical models have substantial biases and ensemble spread.

**Deleted:** Most

80 In recent years, deep learning (DL) methods have been widely used for Arctic sea ice prediction at various temporal scales (e.g., Chi and Kim, 2017; Fritzner et al., 2020; Kim et al., 2020; Y. Ren and X. Li, 2021). Andersson et al. (2021) introduced IceNet to predict probabilities of Arctic sea ice edge with uncertainty quantification. Y. Ren and X. Li (2023) developed a DL

**Deleted:** D

**Deleted:** has

95 method with a physically constrained loss function to improve Arctic sea ice predictions at lead times of 90 days. **However**,  
very limited effort has been made to apply DL methods to Antarctic sea ice prediction and associated assessments are still at  
an early stage. For the SIPN South summer Antarctic sea ice extent forecast (Massonnet et al., 2023), one contributor provided  
the prediction using a k-nearest neighbors (KNN) method. Recently, Wang et al. (2023) developed a SIPNet model with  
encoder-decoder structure for subseasonal Antarctic sea ice concentration prediction, which outperforms some **dynamical**  
100 models and advanced linear statistical models. **Nevertheless, these** DL methods were trained by pure historical sea ice  
concentration data without considering underlying physical processes governing the variation of Antarctic sea ice.  
The purposes of this study are to 1) develop a DL model, named ANTSIC-UNet, to achieve extended seasonal prediction of  
Antarctic sea ice concentration by considering not only **the** sea ice itself but also a wealth of **variables associated with** ocean-  
ice-atmosphere interactions, 2) assess the predictive skill of ANTSIC-UNet for both Pan- and regional Antarctic sea ice,  
105 especially **for** recent extreme years, and 3) **apply** a post-hoc interpretation method to quantify the variable importance that  
affects sea ice predictability.

## 2 Data and Method

### 2.1 Data

In this study, monthly Antarctic sea ice concentration (SIC) data obtained from the National Snow and Ice Data Center  
110 (NSIDC) (<https://nsidc.org/data/nsidc-0079/versions/3>) **are** used as the input of ANTSIC-UNet, **and are** derived from  
brightness temperature of the Scanning Multichannel Microwave Radiometer (SMMR), the Special Sensor Microwave/Imager  
(SSM/I) sensors, and the Special Sensor Microwave Imager/Sounder (SSMIS). The SIC data **have** a size of **332×316 grid**  
115 **points** with a spatial resolution of 25km, spanning from 1979 to 2023. **A linear least-squares trend was fit to observed SIC over**  
**the past 30 years at each grid cell for each calendar month and used to predict SIC values for the corresponding calendar month**  
**in the following year. In addition, these SIC predictions from this linear trend model are also used as the input of ANTSIC-**  
**UNet.**

Long-term observations are scarce in the Antarctic, which cannot provide the comprehensive and consistent three-dimensional  
and time-evolving gridded field of atmosphere and ocean parameters necessary to understand sea ice changes. Reanalysis  
datasets, which assimilate observations and satellite data, are valuable tools for investigating climate changes in polar regions,  
120 offering multivariate descriptions of atmospheric and oceanic conditions. ECWMF Reanalysis v5 (ERA5, Hersbach et al.,  
2020) provides high-resolution and three-dimensional gridded data of comprehensive atmospheric variables from 1940 to the  
present. ERA5 and its predecessor ERA-Interim are widely regarded as the best-performing reanalysis datasets in polar regions,  
with particularly reliable analyses over the Southern Ocean compared with surface and upper-level observations (Bracegirdle  
& Marshall, 2012; Bromwich et al., 2011). Ocean Reanalysis System 5 (ORAS5, Zuo et al., 2019) is a global eddy-permitting  
125 ocean and sea-ice ensemble reanalysis which provides historical ocean and sea-ice conditions from 1979 to the present, and is  
based on the assimilation of the same sea surface temperature observations as is the case of ERA5. Sea ice changes are strongly

**Deleted:** In contrast

**Deleted:** Both the

**Deleted:** knowledge in terms of

**Deleted:** conduct

**Deleted:** is

**Deleted:** which

**Deleted:** s

**Deleted:** 316 × 332

**Deleted:** We also use the linear trend prediction of SIC as the input  
which is computed by the linear least squares fitting for the calendar  
month corresponding to the period of 1-year ahead from the target  
month....

140 influenced by the atmosphere above and the ocean below through dynamical and thermodynamic processes. Therefore, the relevant atmospheric variables selected from ERA5 and oceanic variables obtained from ORAS5 are also used as inputs by ANTSIC-UNet to investigate the key factors contributing to sea ice predictions in the complex interaction between sea ice, ocean and atmosphere. These variables include 2m air temperature (T2), 500-hPa air temperature (T500), sea surface temperature (SST), ocean temperature (PT), ocean heat content for the upper 300m (OHC300), downwelling solar radiation (DSR), upwelling solar radiation (USR), sea level pressure (SLP), 500-hPa geopotential height (H500), 250-hPa geopotential height (H250), 10m u-component of wind (U10), 10m v-component of wind (V10), and 10-hPa zonal wind (U10hPa). The averaged ocean temperature at different depths in the upper Southern Ocean, 50-100m (PT50) and 100-150m (PT100), has been calculated. Before integrating into ANTSIC-UNet, these variables are bilinearly interpolated to the NSIDC sea ice polar stereographic grid and normalised. Additionally, a land mask obtained from the NSIDC is used for the consistency of SIC and other variables.

145 150 The input vector is a 3-dimensional matrix with the size of 332×316×57. The dimension with 57 elements represents all variables mentioned above, including sea ice concentration for the past 12 months, the linear trend prediction of sea ice concentration for the following 6 months, 12 climate variables for the past 3 months, 2 climate variables for the past 1 month, and the land mask. All variable fields are mapped on 332×316 grids (see Table 1 for the details of all input variables). The final output provides the 6-month forecast of Antarctic sea ice concentration.

## 155 2.2 ANTSIC-UNet model

In this study, we construct an ensemble deep learning model, aiming at providing seasonal six-months Antarctic sea ice concentration prediction. The ANTSIC-UNet consists of 20 members possessing the encoder and decoder structure associated with a fully convolutional network (Fig. 1). A U-shaped architecture based on convolutional neural networks is widely used for many applications, i.e., remote sensing image segmentation tasks (Marmanis et al., 2016; Wang et al., 2023). Recently,

160 Andersson et al. (2021) employed the U-Net for three-class predictions of Arctic sea ice concentration.

For accurate forecasts of Antarctic sea ice concentration, we made necessary modifications to the original architecture of U-Net and turned it into single value regression rather than the classification. The ANTSIC-UNet's inputs are feature maps of high-resolution sea ice concentration and other multiple climate variables related to sea ice changes over different lead/lag months and a land mask. The outputs are high-resolution sea ice concentration maps for the future months. To avoid deformation, we resize the spatial shape to a 336×320 grid, by applying the nearest neighbor method, before input to the encoder, and we adopt a padding technique to avoid too much data reduction. The inputs are processed into a large number of feature maps with decreased dimensionality by the encoder part of ANTSIC-UNet. Such deep layers and large-scale features allow the model to capture complex nonlinear relationships and provide an interpretation of the inputs. The decoder then upscales the feature maps extracted by the encoder into upsampled features and uses four skip connections to combine them with multi-scale features from different scale levels of the encoder. This process results in high-resolution output maps that align with the spatial dimensions of the input data. Finally, sigmoid activation functions are used in the last six convolutional

**Deleted:** The atmospheric and oceanic variables obtained from the ECWMF Reanalysis v5 (ERA5, Hersbach et al., 2020) and Ocean Reanalysis System 5 (ORAS5, Zuo et al., 2019) are also used as the inputs, which are related to dynamic and thermodynamic processes of Antarctic sea ice.

**Deleted:** standardized

**Deleted:** 316×332×57

**Deleted:** is the dimension of the

**Deleted:** ,

**Deleted:** 14 climate variables for the past 1 to 3 months

**Deleted:** 316×332

**Deleted:** the

**Deleted:** extended

**Deleted:** Such encoder and decoder framework is also employed in IceNet used for Arctic probabilistic forecasting (Andersson et al., 2021), and originally designed in the U-Net for image recognition (Ronneberger et al., 2015). The encoder is designed to extract abstract features through convolutional layers and downscale features using maxpooling layers, which increases the robustness and reduces the amount of computation for a deeper network. The decoder is designed to recover and reconstruct the abstract features through convolutional layers, and generate outputs of the same spatial size as the inputs through unsampling layers. Four skip connections linking feature maps in the same semantic level provide multi-scale and multi-level information and retain high-resolution details in the initial convolution process.

layers, and the output module extracts slices with dimensions of  $332 \times 316 \times 6$ , which generate the regression predictions for Antarctic sea ice concentration maps over a six-month period.

200 We divide the data into three groups: the training data from 1979 to 2011, the validation data from 2012 to 2019 (with exclusion years 2014 and 2017), and testing data in 2017, from 2020 to 2023 (anomalously low extent period) and 2014 (record high) for independent evaluation. An early stopping strategy is adopted to avoid overfitting when the performance on the validation data does not improve after 10 epochs as suggested by Prechelt (2012). The testing data do not participate in the training process so that the performance of the testing data provides an independent assessment of ANTSIC-UNet's ability to generalize to new data.

**Deleted:** Finally, we extract the slices from the output module which contains six convolutional layers using the sigmoid activation function to transform output values.

**Deleted:** further estimates the generalization

**Deleted:** for adapting

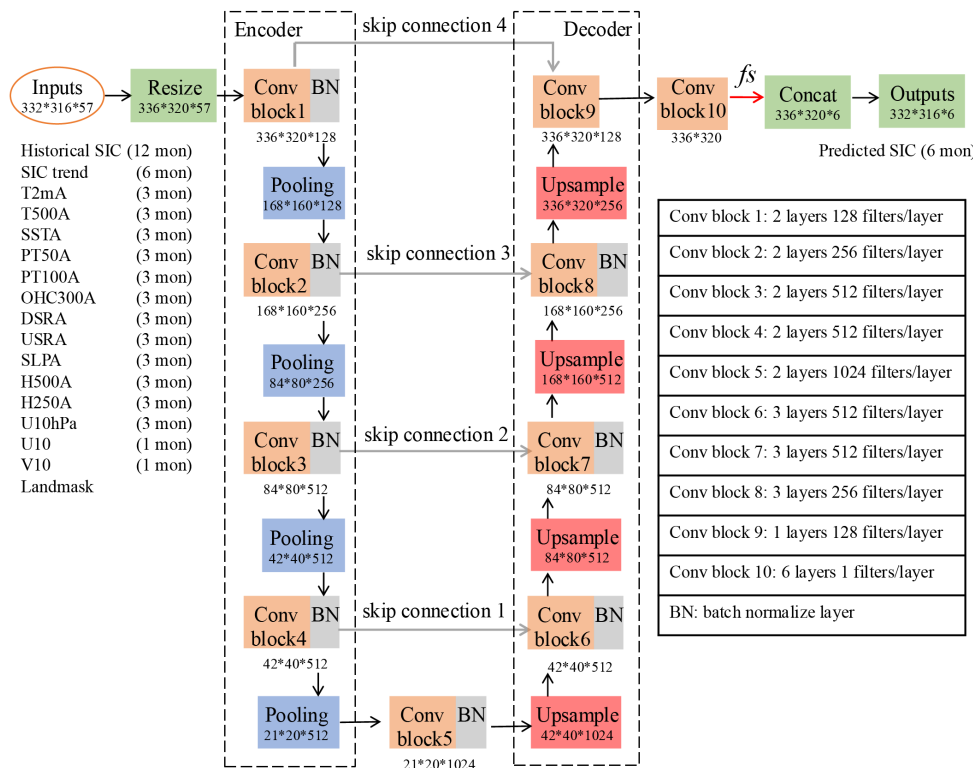


Figure 1. Configuration of ANTSIC-UNet model used for extended seasonal Antarctic sea ice prediction. Inputs are sea ice concentration, other climate variables related to sea ice changes over different lead/lag months and a land mask. The U-shaped

215 architecture includes the encoder, decoder and four skip connections. Sigmoid activation functions (fs) are used in the final six convolutional layers to generate regression predictions of Antarctic sea ice concentration maps for six months.

Input variables	Variable long name	Source	Lead or lag (months)
SIC	sea ice concentration	NSIDC	1 to 12
SIC trend	linear trend forecast for sea ice concentration	NSIDC	1 to 6
T2A	2 m air temperature anomaly	ERA5	1 to 3
T500A	500-hPa air temperature anomaly	ERA5	1 to 3
SSTA	sea surface temperature anomaly	ERA5	1 to 3
PT50A	ocean temperature anomaly averaged over 50-100 m	ORAS5	1 to 3
PT100A	ocean temperature anomaly averaged over 100-150m	ORAS5	1 to 3
OHC300A	ocean heat content anomaly for the upper 300 m	ORAS5	1 to 3
DSRA	surface downward solar radiation	ERA5	1 to 3
USRA	surface upward solar radiation	ERA5	1 to 3
SLPA	sea level pressure anomaly	ERA5	1 to 3
H500A	500-hPa geopotential height anomaly	ERA5	1 to 3
H250A	250-hPa geopotential height anomaly	ERA5	1 to 3
U10hPa	10-hPa zonal wind	ERA5	1 to 3
U10	10 m zonal wind	ERA5	1
V10	10 m meridional wind	ERA5	1
landmask	Southern Hemisphere land mask	NSIDC	N/A

Table 1. The information of all input variables for ANTSIC-UNet

### 2.3 Evaluation metrics

In this study, the linear trend and anomaly persistence predictions are used as benchmarks to assess the predictive skill of  
220 ANTSIC-UNet. The linear trend prediction is described in section 2.1. The anomaly persistence prediction is calculated as follows:

$$SIC_{pred}(t + \tau) = SIC_{clim}(t + \tau) + SIC_{anom}(\tau) \quad (1)$$

where  $SIC_{pred}$  is the target month ice concentration at the lead time  $\tau$ ,  $SIC_{clim}$  is the climatology ice concentration at the target month, and  $SIC_{anom}$  is the observed ice concentration anomaly relative to the climatology at the initial time. The climatology  
225 for each month is computed for the period of the training data (1979-2011). The anomaly persistence works by preserving the deviations from the climatological anomalies and assuming these anomalies will persist into the future. For example, if a

**Deleted:** ,  
**Deleted:**  $\tau$   
**Deleted:** 0,  
**Deleted:**  $\tau$

particular region currently has more sea ice than average, this positive anomaly will continue as time increases. This statistical method has been widely used as a benchmark for predicting sea ice concentration on seasonal timescales since sea ice conditions often change gradually rather than abruptly (Wayand et al., 2019; Bushuk et al., 2021; Niraula and Goessling, 2021). While this method is effective for short-term forecasts, its accuracy declines over longer lead times as the influence of initial anomalies weakens.

235

We quantify the predictive skill of both the Pan- and regional Antarctic sea ice using four metrics: 1) root-mean-square error (RMSE), 2) anomaly correlation coefficient (ACC), 3) mean squared error skill score (MSSS), and 4) integrated ice-edge error (IIEE). RMSE reflects the proximity between the prediction and observation. ACC is a measure of the accuracy of the prediction anomalies based on the relationship between the predicted and observed deviation from their respective 240 climatologies (Wang et al., 2016). MSSS is a skill score based on a comparison between the model predictions and climatology which are considered as a reference forecast. The value of MSSS varies from negative infinity to 1, with a negative value indicating no predictive skill and below the reference forecast (due to deviations from observations being larger than observed 245 annual fluctuations), and 1 indicating a perfect forecast (Murphy, 1988). Here we use ACC = 0.5 and MSSS = 0.0 as the lowest limit for predictive skill, which is widely used in previous research (e.g., Goddard et al., 2012; Choi et al., 2016; Bushuk et al., 2021). The integrated ice-edge error (IIEE) is a verification metric for sea ice forecasts representing the sum of overestimated and underestimated sea ice extent where sea ice concentration > 15% (Goessling et al., 2016). These metrics are calculated as follows:

$$RMSE = \sqrt{MSE} = \sqrt{\text{mean}((p - o)^2)} \quad (2)$$

$$ACC = \frac{\sum(p-p)(o-o)}{\sqrt{\sum(p-p)^2} \sqrt{\sum(o-o)^2}} \quad (3)$$

$$250 \quad MSSS = 1 - \frac{MSE_{pred}}{MSE_{clim}} = 1 - \frac{\sum(p-o)^2}{\sum(o-o)^2} \quad (4)$$

$$IIEE = SIE_p \cup SIE_o - SIE_p \cap SIE_o, \quad (5)$$

where  $p$  is the predicted ice concentration or sea ice extent by ANTSIC-UNet and  $o$  is the observed ice concentration or ice extent;  $p$  and  $o$  are the mean of the prediction and observation.

#### 2.4 Variable importance analysis

255 We use the permutation feature importance approach to determine which variables are important for Antarctic sea ice prediction in ANTSIC-UNet. This method was introduced by Breiman (2001) and Fisher et al. (2018) to interpret the model's decisions. Specifically, when a particular variable is selected, the original input feature matrix is  $X_{orig}$  and the permutation feature matrix is  $X_{perm}$ . The evaluation metric  $e_{i,j}$  used is the root-mean-square error (RMSE) between the output  $f_{i,j}$  (the predicted SIC by the trained model for the target month at the lead time ranging from 1 to 6 months) and the target  $Y_i$  (observed

**Deleted:** model  
**Deleted:** the  
**Deleted:** y  
**Deleted:** of the  
**Deleted:** that takes into account both ACC and conditional bias  
**Deleted:** -1  
**Deleted:** For skillful prediction, h  
**Deleted:** are

**Deleted:**  $\sqrt{\text{mean}(\sum(p - o)^2)}$   
**Deleted:**

270 SIC) for a given month. Thus, the feature importance value  $FI_{ij}$  is defined as the accuracy change of the evaluation metric where  $i$  refers to the target month to be predicted and  $j$  refers to the lead month.

$$FI_{ij} = e_{i,j}^{perm} - e_{i,j}^{orig}, \quad (6)$$

where

$$e_{i,j}^{orig} = RMSE(\mathbf{Y}_i; f_{i,j}(\mathbf{X}_{orig})), \quad (7)$$

275  $e_{i,j}^{perm} = RMSE(\mathbf{Y}_i; f_{i,j}(\mathbf{X}_{perm}))$ . (8)

The importance of each particular variable is measured by 1) randomly shuffling the variable across spatial grids and replacing it in the original input vector to generate a new input vector, and 2) calculating the error of the evaluation metric after permuting the variable. The positive increase of  $FI_{ij}$  means that the variable is important, and no change and decrease of  $FI_{ij}$  indicates that the variable plays little role. Here we iteratively shuffle each input variable and compare the performance, and repeat the procedure 10 times. The mean feature importance value is calculated with the testing data for the period of 2020-2023.

280

### 3 Results

#### 3.1 Pan-Antarctic and regional predictive skill

Pan-Antarctic sea ice concentration predictions from ANTSIC-UNet, linear trend and anomaly persistence models for the testing years averaged for all lead times are shown in Table 2. Overall, ANTSIC-UNet has smaller RMSEs and significantly

285 reduced IIEE compared to the linear trend and anomaly persistence models. In order to consider the variations of the metrics results with lead times and different regions, we compare the three models for lead times ranging from 1 to 6 months for the

Pan-Antarctic and five sub-regions (Fig. 2). For ANTSIC-UNet and anomaly persistence model, both RMSE and IIEE grow with increasing lead time, reflecting a decrease of predictive skill for the extended seasonal forecast. Compared to the anomaly persistence model, ANTSIC-UNet exhibits significantly lower RMSE over the entire Antarctic and all sub-regions for all lead

290 times, except for the Indian Ocean for lead time exceeding 3 months. In addition, RMSE of ANTSIC-UNet also exceeds the linear trend model when the lead time exceeds 3 months, which is due to the reduced predictive skill in the Indian Ocean,

Pacific Ocean, Amundsen and Bellingshausen Seas. Encouragingly, the IIEE of ANTSIC-UNet is consistently smaller than that of the two benchmark models, though it is comparable to the linear trend model for lead times exceeding 3 months in the Amundsen and Bellingshausen Seas. Overall, ANTSIC-UNet shows high predictive skill in the Weddell and Ross Seas,

295 outperforming the two benchmark models.

	ANTSIC-UNet	Linear trend	Anomaly persistence
RMSE	0.21	0.22	0.23
IIEE	1.68	2.13	2.47

**Deleted:** . By contrast

**Deleted:** ,

**Deleted:** has

**Deleted:** the permutation and evaluation

**Deleted:** for

**Deleted:** Considering

**Deleted:** vary

**Deleted:** as the

**Deleted:** s

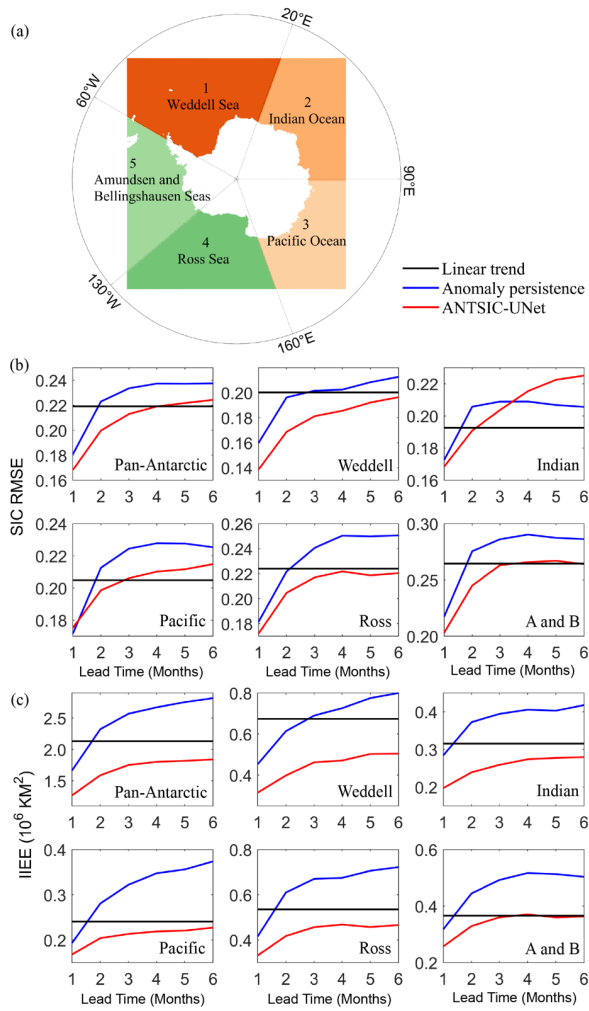
**Deleted:** as

**Deleted:** as

**Deleted:** which

**Deleted:** s

**Table 2. The averaged predictive skill of Antarctic sea ice for ANTSIC-Unet, linear trend and anomaly persistence models for all testing years (RMSE: root-mean-square error; IIEE: integrated ice-edge error).**



315 **Figure 2.** (a) Domian of sub-regions: 60°W–20°E (Weddell Sea), 20°–90°E (Indian Ocean), 90°–160°E (Pacific Ocean), 160°E–130°W (Ross Sea), and 130°–60°W (Amundsen and Bellingshausen Seas). (b) and (c) the averaged predictive skill of Pan- and regional Antarctic sea ice for ANTSIC-UNet, linear trend and anomaly persistence predictions. (b) SIC RMSE and (c) IIEE. Note that the prediction with the linear-trend model is based on the same calendar month one year before and is hence independent of lead time.

Fig. 3 shows the spatial distribution of February and September SIC. In February (seasonal minimum), the linear trend model overestimates SIC in the Ross Sea and western and central Weddell Sea and underestimates SIC in the Amundsen and 320 Bellingshausen Seas. Compared to the linear trend model, the anomaly persistence model has relatively small biases at 1-month lead. However, the magnitude and coverage of the biases become larger as the lead time increases ~~and are~~ large positive (negative) biases in parts of the eastern Pacific sector (the Indian sector) at 5-month lead. Moreover, the anomaly persistence model leads to ~~an unrealistic~~ northward expansion of the biases, as the initial spring months cover a broader area of sea ice t 325 than the target month. By contrast, the ANTSIC-UNet prediction shows the smallest biases (mostly negative ~~across~~ much of the Antarctic) at 1-month lead. As the lead time increases, the magnitude of the biases gradually increases, except that the negative bias in the Ross Sea changes to ~~become~~ positive. In September (seasonal maximum), the linear trend and anomaly persistence (at 1-month lead) models tend to have alternating negative and positive biases near the sea ice edge. By contrast, the ANTSIC-UNet prediction has smaller and mostly negative biases ~~across~~ much of the Antarctic at 1-month lead. As the lead time increases, both the ANTSIC-UNet and anomaly persistence models show biases becoming ~~larger~~ larger in the sea ice edge 330 zone. Moreover, large biases also appear in the compact ice zone for the anomaly persistence model.

Fig. 4 shows spatially and temporally averaged RMSE and IIEE between the ANTSIC-UNet predictions and observations for each target month and different lead times. In terms of RMSE, Pan-Antarctic exhibits low values from autumn to spring (from April to November), though there is an increase in RMSE during summer months (from December to March) as the lead time exceeds 2 months. In terms of IIEE, Pan-Antarctic has small values at 1-month lead, which extend to 2-3 month lead in 335 February and March. In general, the values of IIEE increase as lead times increase, and large values occur from November to January as the lead time exceeds 2-3 months. As shown in Fig. 4b1-f1, the large values of RMSE are also found in summer for all sub-regions, but relatively small values are found in the Weddell Sea. For IIEE in Fig. 4b2-f2, all sub-regions show similar distributions, except that the low IIEE in the Indian and Pacific Oceans have broader coverage. Increased IIEEs are found in the Weddell Sea (Ross Sea) from November to January (from December to March) as the lead time exceeds 2-3 340 months. Overall, the Pacific and Indian Oceans show better predictive skills at the sea ice edge zone in summer relative to other regions.

**Deleted:** , i.e., it shows

**Deleted:** the

**Deleted:** fake

**Deleted:** due to sea ice during the initial months (i.e., spring) having broader coverage

**Deleted:** (i.e., summer) as the lead time increases

**Deleted:** in

**Deleted:** the

**Deleted:** for

**Deleted:** e

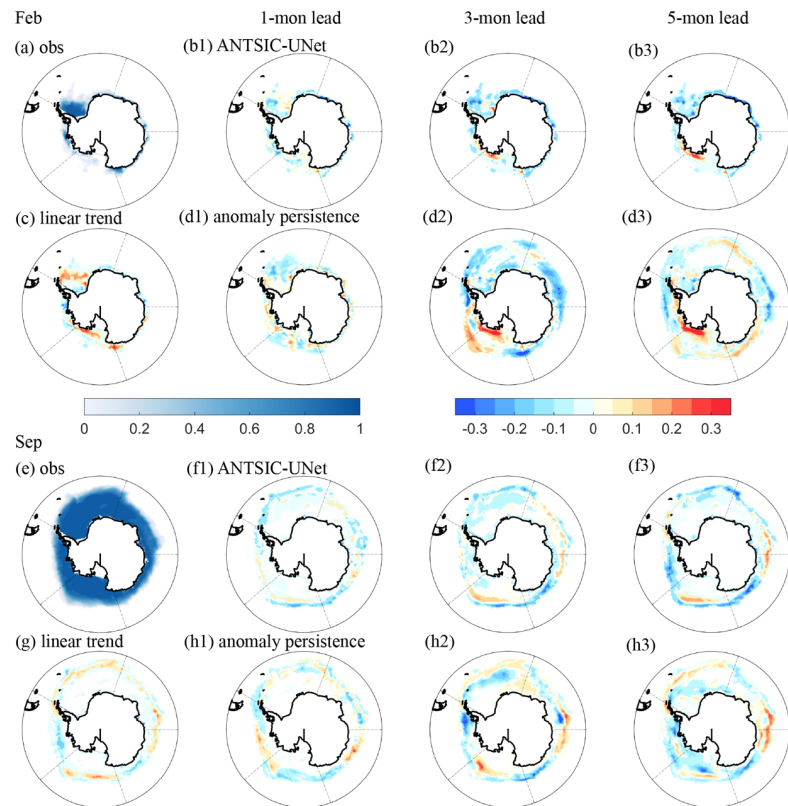


Figure 3. The monthly mean sea ice concentration of the NSIDC observations for (a) February and (e) September, and the errors in predicting by ANTSIC-UNet (b1-b3, f1-f3), the linear trend model (c and g), and anomaly persistence model (d1-d3, h1-h3) at lead time of 1, 3, and 5 months for February (upper panel) and September (lower panel) during the testing years.

355

**Deleted:** predicted

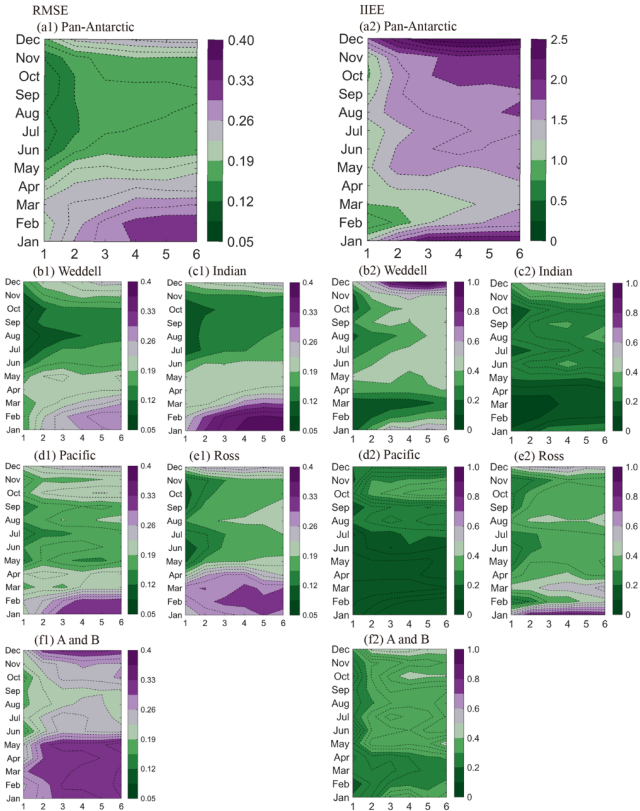


Figure 4. The predictive skill of sea ice concentration (spatially and temporally averaged during the testing years) in terms of RMSE and IIEE (units: million square kilometers) between the ANTSIC-UNet predictions and NSIDC observations for different target months and forecast lead times.

360

### 3.2 Predictive skill for interannual variability

We assess the performance of the predicted year-to-year variability of Pan-Antarctic and regional sea ice extent (SIE) anomalies (Fig. 5). For the Pan-Antarctic, the observed ice extent anomaly shifts from the positive phase to the negative phase around 2016 (Fig. 5a). Both the linear trend and anomaly persistence models cannot capture the observed shift after 2016, and 365 the anomaly persistence model shows much larger positive anomalies and variability compared to the observation. By contrast, ANTSIC-UNet reproduces the observed shift during 2014-2017 and the predicted interannual variability is well correlated

with the observation ( $R=0.76$ ). Moreover, the majority of the observed ice extent anomalies fall within the spread of the ANTSIC-UNet prediction, which is also true for most sub-regions (Fig. 5b-f). The highest correlation is found in the Weddell Sea ( $R=0.79$ ), followed by the Indian Ocean ( $R=0.63$ ) and Ross Sea ( $R=0.59$ ). The Pacific Ocean, Amundsen and 370 Bellingshausen Seas have relatively low correlations. Thus ANTSIC-UNet outperforms two benchmark models from the perspective of the SIE interannual variability prediction.

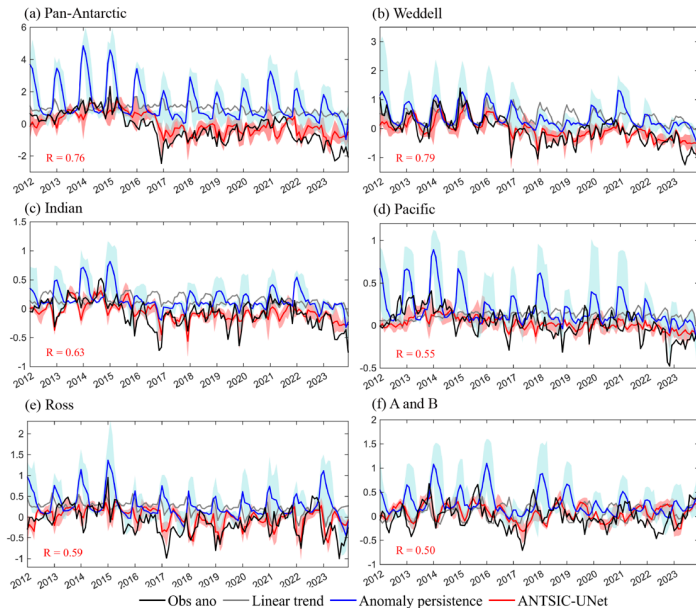


**Figure 5. Sea ice extent anomalies from 2012 to 2023 (including both validation and testing years) for Pan- and regional Antarctic for NSIDC observations (black), the linear trend model (grey), the anomaly persistence model (blue) and ANTSIC-UNet model (red). The red (blue) shading represents the ensemble spread of ANTSIC-UNet (anomaly persistence model) at different lead times up to 6 months, while the solid lines corresponding to the ensemble means. (units: million square kilometers)**

375

Fig. 6 further shows the evaluation metrics (ACC and MSSS) between the observed and predicted interannual sea ice extent. For the Pan-Antarctic, high values of ACC are found from January to September at 1-3 months lead, which decrease as the lead times increase (Fig. 6a). Reduced values of ACC are found from October to December as the lead time exceeds 2 months. 380 MSSS exhibits a similar pattern as that of ACC (Fig. 6b). All sub-regions show similar distributions, high values of ACC and MSSS at 1-month lead and slowly decreasing with increasing lead times. Low values of ACC and MSSS occur in the Indian Ocean from January to March, the Pacific Ocean from November to January, and the Amundsen and Bellingshausen Seas from

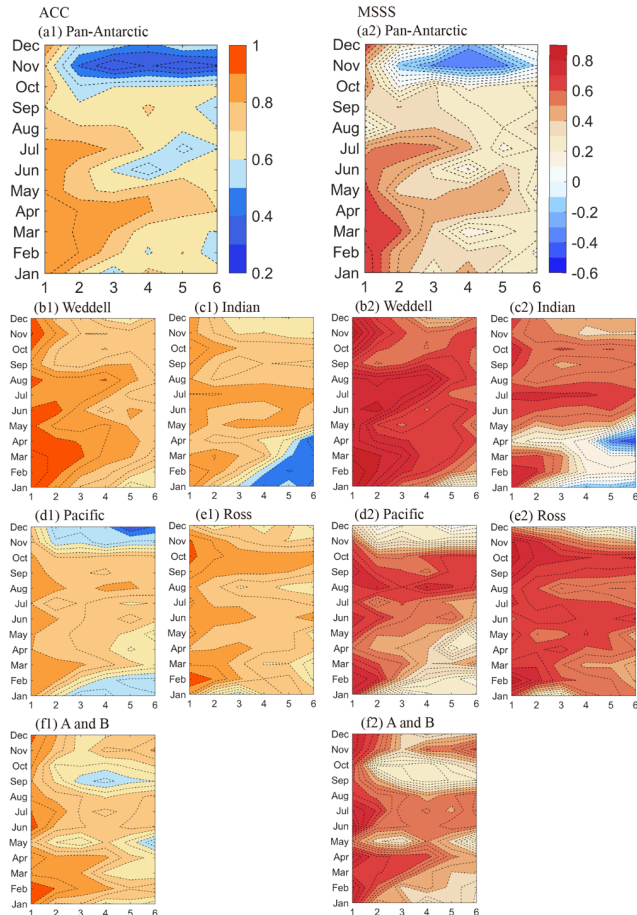
**Deleted:** Time series of s

**Deleted:** .

**Deleted:** The

**Deleted:** lead time averaged predictions are represented by black, grey, blue and red lines

September to October, which limit the interannual predictive skill of the Pan-Antarctic. Overall, the Weddell and Ross Seas have broad coverage of high ACC and MSSS which suggests the possibility of long-lead extended seasonal predictions there.



390

**Figure 6.** The ACC (a1-f1) and MSSS (a2-f2) between the observed and ANTSIC-UNet predicted regional SIE anomalies for different target months and forecast lead times during 1981-2023.

### 3.3 Extreme cases

**Deleted:** Extremes

Next, we evaluate to what extent the ANTSIC-UNet prediction can capture extreme years. The average predictive skills for 395 the three extremely low sea ice extent years averaged for all lead times are shown in Table 3. During all extreme years, ANTSIC-UNet exhibits the smallest RMSEs and improves sea ice edge predictions with notably reduced IIEE, compared to the linear trend and anomaly persistence models. The spatial distribution of February and September SIC of 2023 (record low) is shown in Fig. 7. In February, the linear trend model overestimates sea ice concentration for much of the Antarctic. The anomaly persistence model shows clusters of large positive biases near the coastal area and extended northward coverage of 400 negative biases at 1-month lead, and both magnitude and coverage of the biases increase dramatically as the lead time increases. ANTSIC-UNet exhibits better performance than the two baseline models with smaller sea ice edge error for all lead times, though as lead time increases, the positive biases in the Amundsen and Ross Seas gradually increase. In September, the ANTSIC-UNet prediction shows smaller biases in the entire Antarctic at 1-month lead compared to the two benchmark models, and still outperforms the two models in most regions as the lead time increases. Though there are different spatial distributions 405 of SIC errors for 2017 and 2022, ANTSIC-UNet also shows superior predictive skill (Figs. S1 and S2).

The predictive skill of seasonality errors of extremely low sea ice extent of 2023 based on ANTSIC-UNet and two benchmark models are further accessed against the NSIDC observations (Fig. 8). Both the linear trend and anomaly persistence prediction models excessively overestimate the SIE in the Pan-Antarctic and all sub-regions for nearly all months, except for the Amundsen and Bellingshausen Seas. In contrast, these positive SIE errors have been greatly reduced in the ANTSIC-UNet 410 predictions. ANTSIC-UNet outperforms the linear trend model throughout the year for all the lead times and most regions, except for the Amundsen and Bellingshausen Seas. This is also true for 2017 and 2022 (Figs. S3 and S4). Therefore, ANTSIC-UNet has good predictive skills for extreme events in recent years.

	Observed SIEA	Metrics	ANTSIC-UNet	Linear trend	Anomaly persistence
2017	-0.76	RMSE	0.21	0.25	0.24
		IIEE	1.80	2.56	2.52
2022	-0.84	RMSE	0.21	0.22	0.23
		IIEE	1.68	2.24	2.45
2023	-1.14	RMSE	0.24	0.27	0.31
		IIEE	2.00	3.05	3.11

415 **Table 3.** The averaged predictive skill of ANTSIC-UNet, linear trend and anomaly persistence models for the extreme summer years of Antarctic sea ice. Here, Observed SIEA represents February monthly anomalies of sea ice extent from NSIDC observations for these extreme years, calculated by subtracting the February average sea ice extent for the period 1981-2011 (units: million square kilometers). RMSE: root-mean-square error; IIEE: integrated ice-edge error.

**Deleted:**

... [1]

**Deleted:** the extremely low sea ice extent years

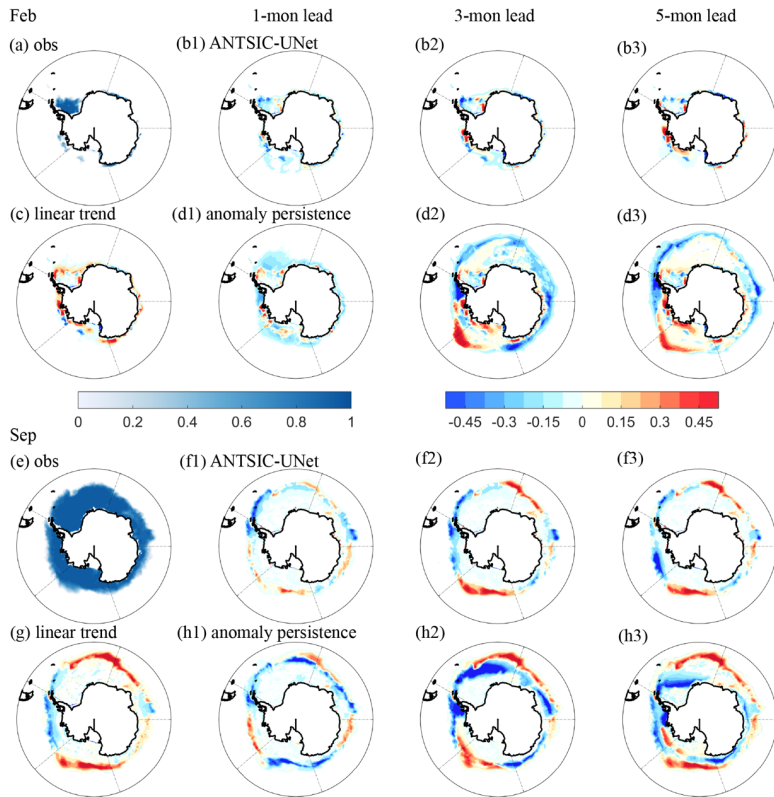
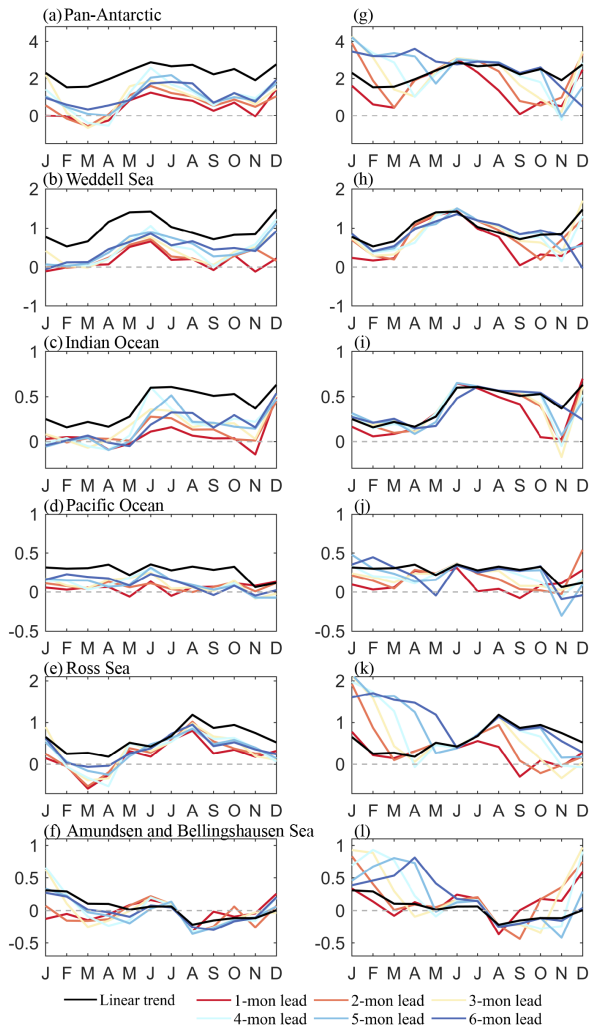


Figure 7. February and September SIC 2023 of NSIDC observations (a, e) and errors predicted by the linear trend model (c, g), anomaly persistence model (d1-d3, h1-h3) and ANTSIC-UNet (b1-b3, f1-f3) at lead time of 1, 3 and 5 months (lowest sea ice extent on record).

Deleted: for 2023



**Figure 8. Seasonality errors of the Pan- and regional Antarctic monthly mean SIE (SIC  $> 15\%$ ) between NSIDC observations and ANTSIC-UNet (a-f) and anomaly persistence model (g-l) predictions at different lead times for 2023 (lowest sea ice extent on record). The black lines show the seasonality SIE errors between observations and linear trend model. (units: million square kilometers)**

### 3.4 Variable importance

In this study, 14 atmospheric and oceanic variables from ERA5 and ORAS5 are selected to capture the key physical mechanisms influencing sea ice variation. Variables such as sea surface temperature, 2m air temperature, and radiation impact heat flux exchanges at the air-ice-sea interface (Bourassa et al., 2013). Near surface winds drive sea ice movement and large-

435 scale tropospheric circulation impacts sea ice through its effects on winds, temperature, precipitation, and cloud cover (Raphael and Hobbs, 2014). The 10-hPa zonal wind represents stratospheric zonal circulation, which impacts surface circulation through downward propagation, influencing sea ice dynamics (Cordero et al., 2023). Sea temperature anomalies and the upper-ocean

heat content anomaly for the upper 300 m taken from ORAS5 play a crucial role in the heat energy exchange at the ocean–ice interface (Purich and Doddridge, 2023; Bianco et al., 2024). The upwelling of warmer subsurface water can further influence

440 sea ice formation and melting in the high latitude of the Southern Ocean (Cai et al., 2023). As discussed, ANTSIC-UNet shows better performance compared to the linear trend and anomaly persistence models. This implies that ANTSIC-UNet has learned

to predict extended seasonal Antarctic sea ice based on the physical relationships of the input variables.

Previous studies suggested that the evaluation metrics of model's predictive skill, especially for models with strong generalization ability, correlate closely with feature importance (FI) (Andersson et al., 2021; Molnar, 2019). The permutation

445 feature importance method based on testing variables can reveal model-dependence variables and indicate the contribution extent of the variables to the performance of the model on unseen data. Here we use the permutation feature-importance method

to explain model variance based on the testing data from 2020–2023. The variable importance is Pan-Antarctic averaged for all calendar months (Fig. 9), and indicates that ANTSIC-UNet is gaining skills from some important variables, including sea

450 ice conditions, sea surface temperature, radiative flux, and stratospheric wind. ANTSIC-UNet also ignores some peripheral variables, such as sea level pressure and subsurface ocean temperature. At short lead times, on timescales of up to two months,

ANTSIC-UNet relies more on the initial sea ice state and linear trend prediction, as well as the surface upward shortwave radiation, sea surface temperature, atmospheric conditions in the troposphere, and 10-hPa zonal wind in the stratosphere. This

implies that ANTSIC-UNet has learned the dynamic and thermodynamic physical mechanisms directly forcing sea ice variations (Son et al., 2009; Turner et al., 2016). At longer lead times, in addition to historical SIC conditions and linear trend

455 predictions of SIC at the target month, the 10-hPa zonal wind stands out as an important influencing factor which manifests

the lagged response in Antarctic sea ice to changes in stratospheric circulation. (Raphael and Hobbs, 2014; Wang et al., 2021).

When a variable shows minimal or even negative importance, it suggests that the ANTSIC-UNet might be overlooking that

feature or has not yet fully captured the intrinsic relationships involving that variable. It may also be related to the accuracy of

the reanalysis data used as input. For example, the lack of predictive importance for downward solar radiation could be due to

460 this variable being poorly represented in the Southern Ocean within the reanalysis as discussed above. Thus, it is crucial to

consider the accuracy of input variables chosen from reanalysis data for Antarctic sea ice predictions.

**Moved (insertion) [1]**

**Deleted:** above

**Deleted:** the

**Deleted:** of a particular model with excellent

**Deleted:** are strongly correlated to

**Deleted:** data

**Deleted:** help us to figure out the

**Deleted:** explain

**Moved up [1]:** As discussed above, ANTSIC-UNet shows better performance compared to the linear trend and anomaly persistence models. This implies that ANTSIC-UNet has learned to predict extended seasonal Antarctic sea ice based on the physical relationships of the input variables.

**Deleted:** feature

**Deleted:** measurement

**Deleted:** results of the

**Deleted:** has learned to use

**Deleted:** has

**Deleted:** learned to

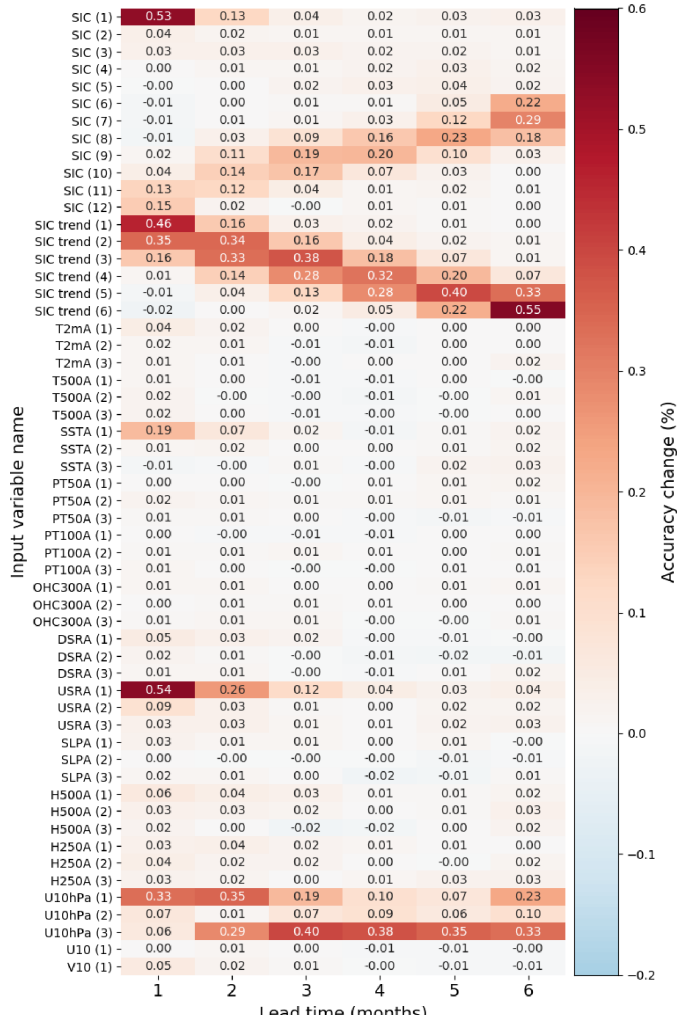


Figure 9. The results of variable importance analysis for Pan-Antarctic based on the permutation feature importance measurement (see Table 1 for full name of the variables).

#### 4 Discussion and Conclusion

485 Antarctic sea ice extent exhibits significant variability driven by the complex air-ice-sea interactions that are not yet fully understood. Sea ice concentration is the essential variable for investigating the variation of sea ice (i.e., extent) and the satellite observation provides long-term reliable records of the data since the late 1970s. In this study, we have introduced a deep learning model, ANTSIC-UNet, to predict the extended seasonal Antarctic monthly-mean sea ice concentration. Considering the complex physical processes influencing Antarctic sea ice variability, in addition to sea ice itself also related atmospheric and oceanic variables are used for ANTSIC-UNet's forecasts. We compare the deep learning predictions against two

490 benchmark models, the linear trend and anomaly persistence models, to evaluate the predictive skill of both Pan- and regional Antarctic sea ice. ANTSIC-UNet exhibits superior predictive skill for Antarctic sea ice for at least 6 months lead, and provides particularly improved predictions of extreme low sea ice events in recent years. The prediction performance of ANTSIC-UNet shows pronounced seasonality and regional dependence, which affects the predictive skill of the Pan-Antarctic. Specifically, during the autumn to spring, low RMSE are observed for most sub-regions. However, increased RMSE is evident in summer

495 for lead time exceeding 2 months indicating decreased model performance in that season. Small values of integrated ice-edge error (IIEE) are found in summer at 1-3 months lead, but large errors occur from November to January as the lead time exceeds 2-4 months. Low RMSE and broader coverage of small IIEE suggest superior predictive skills in the Pacific and Indian Oceans at the sea ice edge zone in summer.

500 We further assess the prediction performance for year-to-year variability. ANTSIC-UNet shows good predictive skill in capturing the interannual variability of Pan-Antarctic and regional sea ice extent anomalies. Consistently high values of ACC and MSSS seen in the Weddell and Ross Seas encouragingly suggest the possibility of performing long-lead extended seasonal predictions. Moreover, the results from the variable importance analysis, computed by a post-hoc interpretation method, suggest that ANTSIC-UNet has learned important relationship between the sea ice and other climate variables having varying impacts across different lead times. Specifically, at short lead times, ANTSIC-UNet predictions are sensitive to initial

505 conditions and linear trend predictions of SIC, sea surface temperature, radiative flux and vertical atmospheric circulation conditions. At longer lead times, predictions are dependent on historical conditions and linear trend predictions of SIC, and stratospheric circulation patterns. The issue that Amundsen and Bellingshausen Seas have the lowest predictive skill might be associated with that ANTSIC-UNet ignoring the sea level pressure and hence the tropical teleconnection relationship associated with the strengthening of Amundsen Sea Low (ASL) in recent decades (Li et al., 2021; Cai et al., 2023).

510 In addition, the ANTSIC-UNet model is trained based on minimizing the loss function which measures the difference between the output and the desired targets. We optimize ANTSIC-UNet using the mean square error (MSE) of SIC as its original loss function. However, the pronounced prediction errors often occur in the vicinity of the sea ice edge, likely associated with oceanic influence and wind dynamics. Interestingly, Y. Ren and X. Li (2023) suggested that the normalized integrated ice-edge error loss might be suitable for long sequence SIC predictions. The question is whether a physically constrained loss

515 function in deep learning models can improve the extended seasonal forecast of Antarctic sea ice. Here we test a hybrid loss

**Deleted:** not only

**Deleted:** but

**Deleted:** extent

**Deleted:** leads to the limitation of

**Deleted:** as the

**Deleted:** s

**Deleted:** the

**Deleted:** The l

**Deleted:** ,

**Deleted:** the

**Deleted:** model-dependence

**Deleted:** with

**Deleted:** es

**Deleted:** and does not consider the relationships of

**Deleted:** and

**Deleted:** at

**Deleted:** which might be

function combining MSE and IIEE to optimize spatial predictions and minimize sea ice edge errors. IIEE loss is calculated by dividing the difference between the predicted and observed sea ice extent by the sum of SIE where SIC > 0.15% in both the prediction and observation. We assign a weight of 0.05 to the IIEE components for values balance in the hybrid loss [expression \(Eq. 10\)](#). Hence, the two loss functions are calculated as:

$$\text{Original Loss} = \text{MSE} = \text{mean}(\sum(p - o)^2), \quad (9)$$

$$\text{Hybrid Loss} = \text{MSE} + 0.05 \frac{\text{IIEE}}{\text{SIE}_p + \text{SIE}_o}, \quad (10)$$

where  $p$  ( $\text{SIE}_p$ ) is the predicted sea ice concentration (ice extent) by ANTSIC-UNet and  $o$  ( $\text{SIE}_o$ ) is the observed ice concentration (ice extent). For clarity, we denote the original loss (hybrid loss) as subscripts "o" ("h") for distinguish between the ANTSIC-UNet models trained with two different loss functions.

Our results show similar distributions of sea ice edge errors predicted by two ANTSIC-UNet models (Fig. 4 a2-f2 and Fig. 10 a1-f1) with small values of IIEE at 1-month lead and large values from November to January as the lead time exceeds 2-4 months. ANTSIC-UNet\_h trained with the hybrid loss slightly reduces the IIEE for the Pan-Antarctic compared to ANTSIC-UNet\_o, especially in Weddell Ocean, Ross Amundsen and Bellingshausen Seas ( $\sim 0.02\text{-}0.05$  million km $^2$ ). However increased errors occur in these regions as lead time exceeds 3-4 months (Fig. 10 a2-f2).

**Deleted:** . T

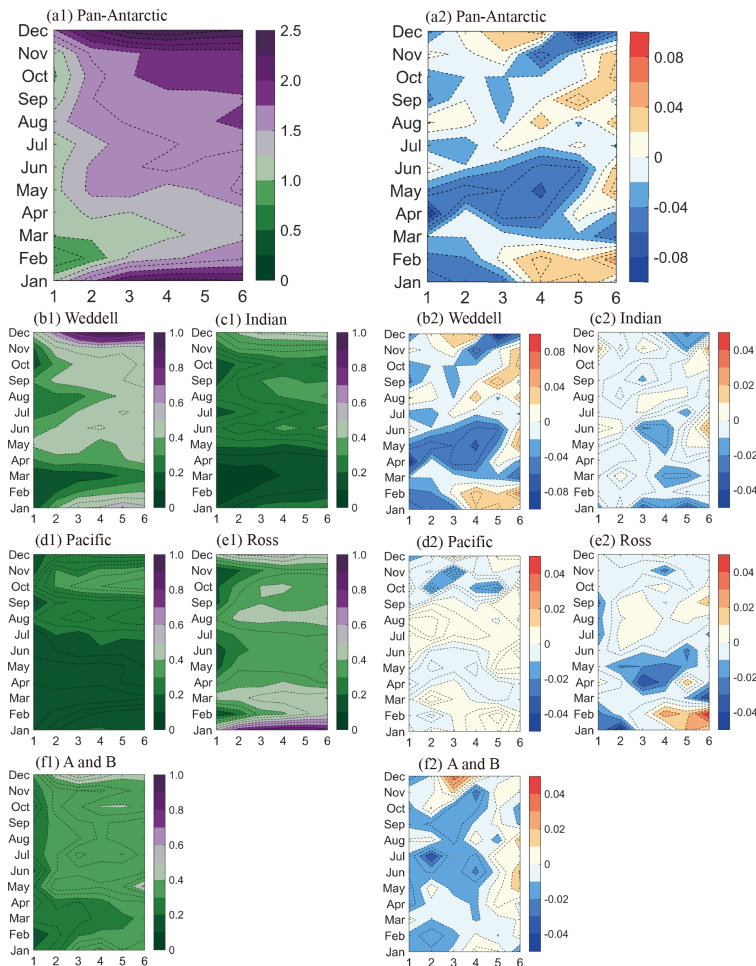
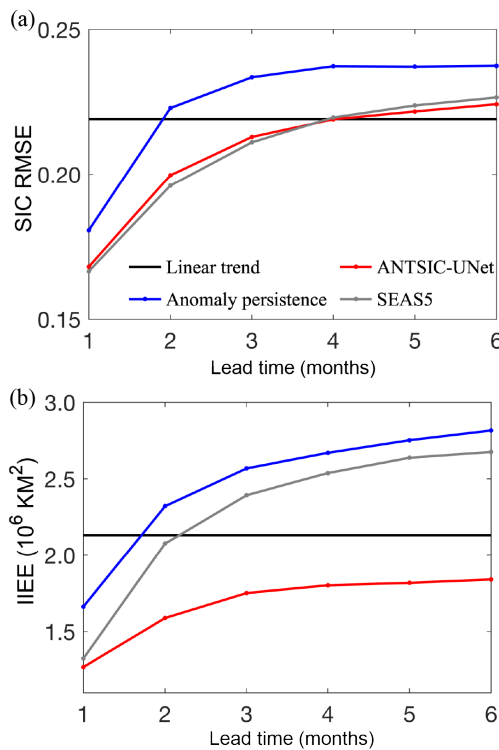


Figure 10. The IIEE of ANTSIC-UNet\_h (a1-f1) and difference (b2-f2) between the two ANTSIC-UNet models trained with different loss functions for different target months and forecast lead times spatially and temporally averaged during the testing years. (units: million square kilometers)

550

To further assess the Antarctic sea ice predictive skill of ANTSIC-UNet against other prediction efforts, we included a dynamical model's monthly mean Antarctic sea ice concentration predictions calculated by the ensemble mean of 51 members

of SEAS5, provided by the Copernicus Climate Change Service (C3S) Prediction project (Thépaut et al., 2018). SEAS5, 555 ECMWF's fifth-generation seasonal forecast system, is recognized for its state-of-art predictive skill among the dynamical models which provides Antarctic sea ice concentration prediction for up to six months (Johnson et al., 2019). As shown in Figure 11, ANTSIC-UNet has small root-mean-square errors (RMSE) for Antarctic sea ice concentration, and outperforms the anomaly persistence predictions at all lead times. Compared to RMSE of SEAS5, those of ANTSIC-UNet are slightly larger errors at 1-3 month lead, and smaller errors as lead time exceeds 4 months, suggesting that the computationally cheaper 560 machine-learning model is highly competitive relative to the dynamical model. In terms of IIEE, ANTSIC-UNet shows significantly superior performance relative to all other models. The superior skills in sea ice edge predictions of ANTSIC-UNet become more pronounced as the lead time increases.



565 **Figure 11.** The average predictive skill of Pan-Antarctic sea ice for ANTSIC-UNet, linear trend, anomaly persistence and SEAS5 predictions during the testing years. (a) SIC RMSE: root-mean-square error and (b) IIEE: integrated ice-edge error.

The past three extreme Antarctic summer SIE events (Table 3) have been linked to key climate drivers and underlying mechanisms. For example, the anomalous sea ice melting during the summer of 2017 might be associated with early spring atmospheric conditions over the Southern Ocean being primarily influenced by a positive phase of the zonal wave 3 (ZW3) pattern, followed by a near-record negative Southern Annular Mode (SAM) (Turner et al., 2017; Schlosser et al., 2018). The 570 significant weakening of the polar stratospheric vortex was identified as a key driver of the SAM changes (Wang et al., 2019). The extremely low sea ice events in the summer of 2022 and 2023 occurred with the deepening of the Amundsen Sea Low (ASL), triggering feedbacks that played a crucial role in the reduction of summer sea ice (Turner et al., 2022; Wang et al., 2022). A few studies have emphasized that the influence of a warm subsurface ocean is a contributor to the recent record-low 575 summer sea ice events (Liu et al., 2023; Purich and Doddridge, 2023). Different large-scale atmospheric circulation patterns may also lead to similar regional prevailing winds, driving the negative Antarctic sea ice extent anomalies (Mezzina et al., 2024).

To our knowledge, little research has focused on the predictability of Antarctic sea ice extent in extreme years. We further compared the ANTSIC-UNet's accuracy performance on sea ice edge predictions for the extreme summer years, relative to linear trend predictions and SEAS5. As shown in Figure 12, both ANTSIC-UNet and SEAS5 have increasing sea ice edge 580 errors as lead time increases. Note again that the linear trend predictions are independent of lead time. ANTSIC-UNet outperforms SEAS5 and linear trend predictions at sea ice edge error in all extreme summer years. At short lead times, ANTSIC-UNet has substantial improvement relative to the linear trend predictions and moderate improvement compared to SEAS5. At long lead times, ANTSIC-UNet's improvements relative to SEAS5 become more significant. These results suggest that ANTSIC-UNet has high predictive skills for extended seasonal predictions of Antarctic sea ice concentration, especially 585 for extreme events, compared to other statistical and dynamical models.

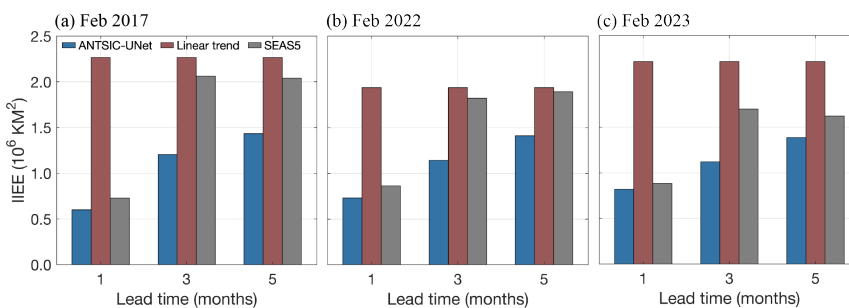


Figure 12. Integrated ice-edge error (IIEE) of ANTSIC-UNet, the linear trend forecast and SEAS5 for February forecasts at lead time of 1, 3, and 5 months for the extreme summer years. (a) 2017, (b) 2022 and (c) 2023.

590 Thus ANTSIC-UNet provides a useful tool for extended seasonal prediction of Antarctic sea ice concentration and extent, and **Deleted:** which also provides valuable information  
for analyzing physical processes important for sea ice variations in different regions. The results from variable importance  
analysis show evidence that ANTSIC-UNet successfully extracts key information from the complex ocean-ice-atmosphere  
interactions to predict sea ice concentration and capture seasonal variations through different climate variables. This approach  
could be effectively extended to other sea ice variables once the relevant long-term data becomes available (i.e., sea ice  
595 thickness). Existing data on Antarctic sea ice thickness, derived from satellite altimetry missions including the ICESat data  
(from 2003-2008), ICESat-2 data (from late 2018 onward) and CryoSat-2 data (from 2010 onward) remain limited in terms of  
confidence and temporal coverage and are not yet suitable for direct deep learning applications (Hendricks et al., 2018; Kacimi  
and Kwok, 2020; Fons et al., 2023). Additional efforts are needed for refining and integrating these datasets into predictive  
600 models. The Polar Pathfinder product (Tschudi et al. 2019) provides daily sea ice motion vectors at a spatial resolution of 25  
km, which are valuable for investigating sea ice movement patterns under the influence of wind and ocean currents. Future  
research will explore whether incorporating dynamic factors such as ice drift can enhance the accuracy of sea ice predictions.  
In addition, further investigation is also needed based on physically enriched deep learning models**is needed to explore more**  
thoroughly the physical mechanisms between SIC and other climate variables with long-term memory, such as sea ice thickness  
605 and ocean heat content (Marchi et al., 2019; Bushuk et al., 2021; Libera et al., 2022).

605

*Data Availability.* All the data analyzed here are openly available. NSIDC sea ice concentration data is publicly available at <https://nsidc.org/data/nsidc-0079/versions/3>. ERA5 monthly averaged data on pressure levels from 1979 to present is publicly available at <https://cds.climate.copernicus.eu/doi/10.24381/cds.6860a573>. ERA5 monthly averaged data on single levels from 1979 to present is publicly available at <https://cds.climate.copernicus.eu/doi/10.24381/cds.f17050d7>. ORAS5 monthly average data from 1979 to present is publicly available at <https://cds.climate.copernicus.eu/cdsapp#!/dataset/10.24381/cds.67e8eeb7>.

*Author contributions.* JL conceived the study, ZY and JL designed the model, carried out the analysis and wrote the paper; all authors participated in constructive discussions and helped improve the manuscript.

*Competing interests.* The authors declare that they have no conflict of interest.

615 *Acknowledgements.* This research was supported by National Key Research and Development Program of China (Grant No. 2022YFE0106800) and the National Key Scientific and Technological Infrastructure project “Earth System Science Numerical Simulator Facility” (EarthLab).

## Reference

Abernathey, R. P., Cerovecki, I., Holland, P. R., Newsom, E., Mazloff, M., and Talley, L. D.: Water-mass transformation by sea ice in the upper branch of the Southern Ocean overturning, *Nature Geosci*, 9, 596–601, <https://doi.org/10.1038/geo2749>, 620 2016.

Andersson, T. R., Hosking, J. S., Pérez-Ortiz, M., Paige, B., Elliott, A., Russell, C., Law, S., Jones, D. C., Wilkinson, J., Phillips, T., Byrne, J., Tietsche, S., Sarojini, B. B., Blanchard-Wrigglesworth, E., Aksenov, Y., Downie, R., and Shuckburgh,

E.: Seasonal Arctic sea ice forecasting with probabilistic deep learning, *Nature Communications*, 12, 5124, <https://doi.org/10.1038/s41467-021-25257-4>, 2021.

630 [Bianco, E., Iovino, D., Masina, S., Materia, S., and Ruggieri, P.: The role of upper-ocean heat content in the regional variability of Arctic sea ice at sub-seasonal timescales, \*The Cryosphere\*, 18, 2357–2379, <https://doi.org/10.5194/tc-18-2357-2024>, 2024.](#)

Bourassa, M. A., Gille, S. T., Bitz, C., Carlson, D., Cervenka, I., Clayton, C. A., Cronin, M. F., Drennan, W. M., Fairall, C. W., Hoffman, R. N., Magnusdottir, G., Pinker, R. T., Renfrew, I. A., Serreze, M., Speer, K., Talley, L. D., and Wick, G. A.: [High-Latitude Ocean and Sea Ice Surface Fluxes: Challenges for Climate Research, <https://doi.org/10.1175/BAMS-D-11-00244.1>, 2013.](#)

635 [Bracegirdle, T. J. and Marshall, G. J.: The Reliability of Antarctic Tropospheric Pressure and Temperature in the Latest Global Reanalyses, <https://doi.org/10.1175/JCLI-D-11-00685.1>, 2012.](#)

Breiman, L.: Random Forests, *Machine Learning*, 45, 5–32, <https://doi.org/10.1023/A:1010933404324>, 2001.

Bromwich, D. H., Nicolas, J. P., and Monaghan, A. J.: [An Assessment of Precipitation Changes over Antarctica and the Southern Ocean since 1989 in Contemporary Global Reanalyses, <https://doi.org/10.1175/2011JCLI4074.1>, 2011.](#)

640 Bushuk, M., Winton, M., Haumann, F. A., Delworth, T., Lu, F., Zhang, Y., Jia, L., Zhang, L., Cooke, W., Harrison, M., Hurlin, B., Johnson, N. C., Kapnick, S. B., McHugh, C., Murakami, H., Rosati, A., Tseng, K.-C., Wittenberg, A. T., Yang, X., and Zeng, F.: Seasonal Prediction and Predictability of Regional Antarctic Sea Ice, *Journal of Climate*, 34, 6207–6233, <https://doi.org/10.1175/JCLI-D-20-0965.1>, 2021.

645 Cai, W., Jia, F., Li, S., Purich, A., Wang, G., Wu, L., Gan, B., Santoso, A., Geng, T., Ng, B., Yang, Y., Ferreira, D., Meehl, G. A., and McPhaden, M. J.: Antarctic shelf ocean warming and sea ice melt affected by projected El Niño changes, *Nat. Clim. Chang.*, 13, 235–239, <https://doi.org/10.1038/s41558-023-01610-x>, 2023.

Chen, D. and Yuan, X.: A Markov Model for Seasonal Forecast of Antarctic Sea Ice, *Journal of Climate*, 17, 3156–3168, [https://doi.org/10.1175/1520-0442\(2004\)017<3156:AMMFSF>2.0.CO;2](https://doi.org/10.1175/1520-0442(2004)017<3156:AMMFSF>2.0.CO;2), 2004.

650 Chi, J. and Kim, H.: Prediction of Arctic Sea Ice Concentration Using a Fully Data Driven Deep Neural Network, *Remote Sensing*, 9, 1305, <https://doi.org/10.3390/rs9121305>, 2017.

Choi, J., Son, S.-W., Ham, Y.-G., Lee, J.-Y., and Kim, H.-M.: Seasonal-to-Interannual Prediction Skills of Near-Surface Air Temperature in the CMIP5 Decadal Hindcast Experiments, *Journal of Climate*, 29, 1511–1527, <https://doi.org/10.1175/jcli-d-15-0182.1>, 2016.

655 Comiso, J. C., Gersten, R. A., Stock, L. V., Turner, J., Perez, G. J., and Cho, K.: Positive Trend in the Antarctic Sea Ice Cover and Associated Changes in Surface Temperature, *Journal of Climate*, 30, 2251–2267, <https://doi.org/10.1175/JCLI-D-16-0408.1>, 2017.

[Cordero, R. R., Feron, S., Damiani, A., Llanillo, P. J., Carrasco, J., Khan, A. L., Bintanja, R., Ouyang, Z., and Casassa, G.: Signature of the stratosphere-troposphere coupling on recent record-breaking Antarctic sea-ice anomalies, \*The Cryosphere\*, 17, 4995–5006, <https://doi.org/10.5194/tc-17-4995-2023>, 2023.](#)

660 Fisher, A. J., Rudin, C., and Dominici, F.: Model Class Reliance: Variable Importance Measures for any Machine Learning Model Class, from the “Rashomon” Perspective, 2018.

Fogt, R. L., Sleinkofer, A. M., Raphael, M. N., and Handcock, M. S.: A regime shift in seasonal total Antarctic sea ice extent in the twentieth century, *Nature Climate Change*, 12, 54–62, <https://doi.org/10.1038/s41558-021-01254-9>, 2022.

665 [Fritzner, S., Graversen, R., and Christensen, K. H.: Assessment of High-Resolution Dynamical and Machine Learning Models for Prediction of Sea Ice Concentration in a Regional Application, \*Journal of Geophysical Research: Oceans\*, 125, https://doi.org/10.1029/2020jc016277, 2020.](https://doi.org/10.1029/2020jc016277)

Goddard, L., Kumar, A., Solomon, A., Smith, D., Boer, G., Gonzalez, P., Kharin, V., Merryfield, W., Deser, C., Mason, S. J., Kirtman, B. P., Msadek, R., Sutton, R., Hawkins, E., Fricker, T., Hegerl, G., Ferro, C. A. T., Stephenson, D. B., Meehl, G. A., Stockdale, T., Burgman, R., Greene, A. M., Kushnir, Y., Newman, M., Carton, J., Fukumori, I., and Delworth, T.: A 670 verification framework for interannual-to-decadal predictions experiments, *Climate Dynamics*, 40, 245–272, <https://doi.org/10.1007/s00382-012-1481-2>, 2012.

Goessling, H. F., Tietsche, S., Day, J. J., Hawkins, E., and Jung, T.: Predictability of the Arctic sea ice edge, *Geophysical Research Letters*, 43, 1642–1650, <https://doi.org/10.1002/2015GL067232>, 2016.

675 Hersbach, H., Bell, B., Berrisford, P., Hirahara, S., Horányi, A., Muñoz-Sabater, J., Nicolas, J., Peubey, C., Radu, R., Schepers, D., Simmons, A., Soci, C., Abdalla, S., Abellán, X., Balsamo, G., Bechtold, P., Biavati, G., Bidlot, J., Bonavita, M., De Chiara, G., Dahlgren, P., Dee, D., Diamantakis, M., Dragani, R., Flemming, J., Forbes, R., Fuentes, M., Geer, A., Haimberger, L., Healy, S., Hogan, R. J., Hólm, E., Janisková, M., Keeley, S., Laloyaux, P., Lopez, P., Lupu, C., Radnoti, G., de Rosnay, P., Rozum, I., Vamborg, F., Villaume, S., and Thépaut, J.-N.: The ERA5 global reanalysis, *Quarterly Journal of the Royal Meteorological Society*, 146, 1999–2049, <https://doi.org/10.1002/qj.3803>, 2020.

680 Hobbs, W. R., Massom, R., Stammerjohn, S., Reid, P., Williams, G., and Meier, W.: A review of recent changes in Southern Ocean sea ice, their drivers and forcings, *Global and Planetary Change*, 143, 228–250, <https://doi.org/10.1016/j.gloplacha.2016.06.008>, 2016.

Hogg, J., Fonoüberova, M., and Mezić, I.: Exponentially decaying modes and long-term prediction of sea ice concentration using Koopman mode decomposition, *Scientific Reports*, 10, 16313, <https://doi.org/10.1038/s41598-020-73211-z>, 2020.

685 [Johnson, S. J., Stockdale, T. N., Ferranti, L., Balmaseda, M. A., Molteni, F., Magnusson, L., Tietsche, S., Decremer, D., Weisheimer, A., Balsamo, G., Keeley, S. P. E., Mogensen, K., Zuo, H., and Monge-Sanz, B. M.: SEAS5: the new ECMWF seasonal forecast system, \*Geoscientific Model Development\*, 12, 1087–1117, https://doi.org/10.5194/gmd-12-1087-2019, 2019.](https://doi.org/10.5194/gmd-12-1087-2019)

690 Kidston, J., Taschetto, A. S., Thompson, D. W. J., and England, M. H.: The influence of Southern Hemisphere sea-ice extent on the latitude of the mid-latitude jet stream, *Geophysical Research Letters*, 38, <https://doi.org/10.1029/2011GL048056>, 2011.

Kim, Y. J., Kim, H.-C., Han, D., Lee, S., and Im, J.: Prediction of monthly Arctic sea ice concentrations using satellite and reanalysis data based on convolutional neural networks, *The Cryosphere*, 14, 1083–1104, <https://doi.org/10.5194/tc-14-1083-2020>, 2020.

695 Li, X., Cai, W., Meehl, G. A., Chen, D., Yuan, X., Raphael, M., Holland, D. M., Ding, Q., Fogt, R. L., Markle, B. R., Wang, G., Bromwich, D. H., Turner, J., Xie, S.-P., Steig, E. J., Gille, S. T., Xiao, C., Wu, B., Lazzara, M. A., Chen, X., Stammerjohn, S., Holland, P. R., Holland, M. M., Cheng, X., Price, S. F., Wang, Z., Bitz, C. M., Shi, J., Gerber, E. P., Liang, X., Goosse, H., Yoo, C., Ding, M., Geng, L., Xin, M., Li, C., Dou, T., Liu, C., Sun, W., Wang, X., and Song, C.: Tropical teleconnection impacts on Antarctic climate changes, *Nature Reviews Earth & Environment*, 2, 680–698, <https://doi.org/10.1038/s43017-021-00204-5>, 2021.

700 Libera, S., Hobbs, W., Klocker, A., Meyer, A., and Matear, R.: Ocean-Sea Ice Processes and Their Role in Multi-Month Predictability of Antarctic Sea Ice, *Geophysical Research Letters*, 49, e2021GL097047, <https://doi.org/10.1029/2021GL097047>, 2022.

Liu, J., Curry, J. A., and Martinson, D. G.: Interpretation of recent Antarctic sea ice variability, *Geophysical Research Letters*, 31, <https://doi.org/10.1029/2003GL018732>, 2004.

705 Liu, J., Zhu, Z., and Chen, D.: Lowest Antarctic Sea Ice Record Broken for the Second Year in a Row, *Ocean-Land-Atmosphere Research*, 2, 0007, <https://doi.org/10.34133/olar.0007>, 2023.

Marchi, S., Fichefet, T., Goosse, H., Zunz, V., Tietsche, S., Day, J. J., and Hawkins, E.: Reemergence of Antarctic sea ice predictability and its link to deep ocean mixing in global climate models, *Climate Dynamics*, 52, 2775–2797, <https://doi.org/10.1007/s00382-018-4292-2>, 2019.

710 [Marmanis, D., Datcu, M., Esch, T., and Stilla, U.: Deep Learning Earth Observation Classification Using ImageNet Pretrained Networks, IEEE Geoscience and Remote Sensing Letters](#), 13, 105–109, <https://doi.org/10.1109/LGRS.2015.2499239>, 2016.

Massom, R. A. and Stammerjohn, S. E.: Antarctic sea ice change and variability – Physical and ecological implications, *Polar Science*, 4, 149–186, <https://doi.org/10.1016/j.polar.2010.05.001>, 2010.

715 Massonnet, F., Barreira, S., Barthélémy, A., Bilbao, R., Blanchard-Wrigglesworth, E., Blockley, E., Bromwich, D. H., Bushuk, M., Dong, X., Goessling, H. F., Hobbs, W., Iovino, D., Lee, W.-S., Li, C., Meier, W. N., Merryfield, W. J., Moreno-Chamarro, E., Morioka, Y., Li, X., Niraula, B., Petty, A., Sanna, A., Scilingo, M., Shu, Q., Sigmond, M., Sun, N., Tietsche, S., Wu, X., Yang, Q., and Yuan, X.: SIPN South: six years of coordinated seasonal Antarctic sea ice predictions, *Frontiers in Marine Science*, 10, 2023.

720 [Mezzina, B., Goosse, H., Klein, F., Barthélémy, A., and Massonnet, F.: The role of atmospheric conditions in the Antarctic sea ice extent summer minima, The Cryosphere](#), 18, 3825–3839, <https://doi.org/10.5194/tc-18-3825-2024>, 2024.

Molnar, C., 2019: Interpretable Machine Learning. A Guide for Making Black Box Models Explainable. <https://christophm.github.io/interpretable-ml-book/>.

Morioka, Y., Doi, T., Iovino, D., Masina, S., and Behera, S. K.: Role of sea-ice initialization in climate predictability over the Weddell Sea, *Sci Rep*, 9, 2457, <https://doi.org/10.1038/s41598-019-39421-w>, 2019.

725 Murphy, A. H.: Skill Scores Based on the Mean Square Error and Their Relationships to the Correlation Coefficient, *Monthly Weather Review*, 116, 2417–2424, [https://doi.org/10.1175/1520-0493\(1988\)116<2417:SSBOTM>2.0.CO;2](https://doi.org/10.1175/1520-0493(1988)116<2417:SSBOTM>2.0.CO;2), 1988.

[Niraula, B. and Goessling, H. F.: Spatial Damped Anomaly Persistence of the Sea Ice Edge as a Benchmark for Dynamical Forecast Systems, Journal of Geophysical Research: Oceans](#), 126, e2021JC017784, <https://doi.org/10.1029/2021JC017784>, 2021.

730 Pei, Y.: Cyclostationary EOF Modes of Antarctic Sea Ice and Their Application in Prediction, *Journal of Geophysical Research: Oceans*, 126, e2021JC017179, <https://doi.org/10.1029/2021JC017179>, 2021.

[Purich, A. and Doddridge, E. W.: Record low Antarctic sea ice coverage indicates a new sea ice state, Commun Earth Environ](#), 4, 1–9, <https://doi.org/10.1038/s43247-023-00961-9>, 2023.

735 Prechelt, L.: Early Stopping — But When?, in: Neural Networks: Tricks of the Trade: Second Edition, edited by: Montavon, G., Orr, G. B., and Müller, K.-R., Springer Berlin Heidelberg, Berlin, Heidelberg, 53–67, [https://doi.org/10.1007/978-3-642-35289-8\\_5](https://doi.org/10.1007/978-3-642-35289-8_5), 2012.

Raphael, M. N. and Hobbs, W.: The influence of the large-scale atmospheric circulation on Antarctic sea ice during ice advance and retreat seasons, *Geophysical Research Letters*, 41, 5037–5045, <https://doi.org/10.1002/2014GL060365>, 2014.

740 Ren, Y. and Li, X.: Predicting the Daily Sea Ice Concentration on a Sub-Seasonal Scale of the Pan-Arctic During the Melting Season by a Deep Learning Model, *IEEE Transactions on Geoscience and Remote Sensing*, 1–1, <https://doi.org/10.1109/TGRS.2023.3279089>, 2023.

Son, S.-W., Tandon, N. F., Polvani, L. M., and Waugh, D. W.: Ozone hole and Southern Hemisphere climate change, *Geophysical Research Letters*, 36, n/a-n/a, <https://doi.org/10.1029/2009gl038671>, 2009.

745 Schlosser, E., Haumann, F. A., and Raphael, M. N.: *Atmospheric influences on the anomalous 2016 Antarctic sea ice decay*, *The Cryosphere*, 12, 1103–1119, <https://doi.org/10.5194/tc-12-1103-2018>, 2018.

Thépaut, J.-N., Dee, D., Engelen, R., and Pinty, B.: The Copernicus Programme and its Climate Change Service, in: *IGARSS 2018 - 2018 IEEE International Geoscience and Remote Sensing Symposium, IGARSS 2018 - 2018 IEEE International Geoscience and Remote Sensing Symposium*, 1591–1593, <https://doi.org/10.1109/IGARSS.2018.8518067>, 2018.

750 Turner, J., Phillips, T., Marshall, G. J., Hosking, J. S., Pope, J. O., Bracegirdle, T. J., and Deb, P.: Unprecedented springtime retreat of Antarctic sea ice in 2016, *Geophysical Research Letters*, 44, 6868–6875, <https://doi.org/10.1002/2017GL073656>, 2017.

Turner, J., Holmes, C., Caton Harrison, T., Phillips, T., Jena, B., Reeves-Francois, T., Fogt, R., Thomas, E. R., and Bajish, C. C.: Record Low Antarctic Sea Ice Cover in February 2022, *Geophysical Research Letters*, 49, e2022GL098904, <https://doi.org/10.1029/2022GL098904>, 2022.

755 Turner, J., Bracegirdle, T. J., Phillips, T., Marshall, G. J., and Hosking, J. S.: An Initial Assessment of Antarctic Sea Ice Extent in the CMIP5 Models, *Journal of Climate*, 26, 1473–1484, <https://doi.org/10.1175/JCLI-D-12-00068.1>, 2013.

Turner, J., Hosking, J. S., Marshall, G. J., Phillips, T., and Bracegirdle, T. J.: Antarctic sea ice increase consistent with intrinsic variability of the Amundsen Sea Low, *Clim Dyn*, 46, 2391–2402, <https://doi.org/10.1007/s00382-015-2708-9>, 2016.

760 Wang, G., Hendon, H. H., Arblaster, J. M., Lim, E.-P., Abhik, S., and van Renssch, P.: Compounding tropical and stratospheric forcing of the record low Antarctic sea-ice in 2016, *Nat Commun*, 10, 13, <https://doi.org/10.1038/s41467-018-07689-7>, 2019.

Wang, J., Luo, H., Yang, Q., Liu, J., Yu, L., Shi, Q., and Han, B.: An Unprecedented Record Low Antarctic Sea-ice Extent during Austral Summer 2022, *Adv. Atmos. Sci.*, 39, 1591–1597, <https://doi.org/10.1007/s00376-022-2087-1>, 2022.

Wang, L., Yuan, X., Ting, M., and Li, C.: Predicting Summer Arctic Sea Ice Concentration Intraseasonal Variability Using a Vector Autoregressive Model, *Journal of Climate*, 29, 1529–1543, <https://doi.org/10.1175/JCLI-D-15-0313.1>, 2016.

765 Wang, S., Liu, J., Cheng, X., Kerzenmacher, T., Hu, Y., Hui, F., and Braesicke, P.: How Do Weakening of the Stratospheric Polar Vortex in the Southern Hemisphere Affect Regional Antarctic Sea Ice Extent?, *Geophysical Research Letters*, 48, e2021GL092582, <https://doi.org/10.1029/2021GL092582>, 2021.

**Deleted:** Ronneberger, O., Fischer, P., and Brox, T.: U-Net: Convolutional Networks for Biomedical Image Segmentation, in: *Medical Image Computing and Computer-Assisted Intervention – MICCAI 2015*, Cham, 234–241, 2015.<sup>¶</sup>

775 [Wang, X., Hu, Z., Shi, S., Hou, M., Xu, L., and Zhang, X.: A deep learning method for optimizing semantic segmentation accuracy of remote sensing images based on improved UNet, Sci Rep, 13, 7600, https://doi.org/10.1038/s41598-023-34379-2, 2023.](https://doi.org/10.1038/s41598-023-34379-2)

775 Wang, Y., Yuan, X., Ren, Y., Bushuk, M., Shu, Q., Li, C., and Li, X.: Subseasonal Prediction of Regional Antarctic Sea Ice by a Deep Learning Model, Geophysical Research Letters, 50, e2023GL104347, https://doi.org/10.1029/2023GL104347, 2023.

780 [Wang, Z., Turner, J., Sun, B., Li, B., and Liu, C.: Cyclone-induced rapid creation of extreme Antarctic sea ice conditions, Sci Rep, 4, 5317, https://doi.org/10.1038/srep05317, 2014.](https://doi.org/10.1038/srep05317)

785 [Wayand, N. E., Bitz, C. M., and Blanchard-Wrigglesworth, E.: A Year-Round Subseasonal-to-Seasonal Sea Ice Prediction Portal, Geophysical Research Letters, 46, 3298–3307, https://doi.org/10.1029/2018GL081565, 2019.](https://doi.org/10.1029/2018GL081565)

785 Y. Ren and X. Li: Predicting Daily Arctic Sea Ice Concentration in the Melt Season Based on a Deep Fully Convolution Network Model, in: 2021 IEEE International Geoscience and Remote Sensing Symposium IGARSS, 2021 IEEE International Geoscience and Remote Sensing Symposium IGARSS, journalAbbreviation: 2021 IEEE International Geoscience and Remote Sensing Symposium IGARSS, 5540–5543, https://doi.org/10.1109/IGARSS47720.2021.9554118, 2021.

790 Zampieri, L., Goessling, H. F., and Jung, T.: Predictability of Antarctic Sea Ice Edge on Subseasonal Time Scales, Geophysical Research Letters, 46, 9719–9727, https://doi.org/10.1029/2019GL084096, 2019.

790 Zhu, Z., Liu, J., Song, M., and Hu, Y.: Changes in Extreme Temperature and Precipitation over the Southern Extratropical Continents in Response to Antarctic Sea Ice Loss, Journal of Climate, 36, 4755–4775, https://doi.org/10.1175/JCLI-D-22-0577.1, 2023.

Zuo, H., Balmaseda, M. A., Tietsche, S., Mogensen, K., and Mayer, M.: The ECMWF operational ensemble reanalysis–analysis system for ocean and sea ice: a description of the system and assessment, Ocean Science, 15, 779–808, https://doi.org/10.5194/os-15-779-2019, 2019.